

## Supplementary material

Here we present the supplementary material to the article “Inherent noise can facilitate coherence in collective swarm motion”, submitted to PNAS.

### S.1 Derivation of the formula [11]

Consider the Fokker-Planck equation [7]

$$\frac{\partial f_N}{\partial t} = \frac{\partial}{\partial U} \left( \frac{\omega^2}{24N} \frac{\partial f_N}{\partial U} - \{G(U) - U\} f_N \right). \quad (\text{S.1})$$

Let  $T$  be the time in which the alignment leaves  $(-\infty, 0)$  if initialized at  $U_-$  when  $t = 0$ . For  $n > 0$  we define the  $n^{\text{th}}$  moment for the distribution of the escape time,  $T$ , by  $T_n = \langle T^n \rangle$ . It can be shown (for the specific FPE [7], describing escape from a potential well subject to weak intensity additive noise, but not for every single FPE), as in (1) for example, that

$$T_1 = \frac{24N}{\omega^2} \int_{U_-}^0 \exp[\phi_N(U)] \int_{-\infty}^U \exp[-\phi_N(\xi)] d\xi dU, \quad (\text{S.2})$$

where the potential  $\phi_N(U)$  is given by Eq. [9] in the main text, namely,

$$\phi_N(U) = \frac{12N\beta}{\omega^2(1+\beta)} [U^2 - 2|U|]. \quad (\text{S.3})$$

Notice that Eq. (S.2) is Eq. [10] in the main text. To approximate the inner integral in (S.2) we can move the upper bound from  $U$  to zero (since, over the region we are integrating, most of the weight of the integrand is concentrated around the minimum of the potential,  $U_-$ ) allowing the separation of the integrals,

$$T_1 \approx \frac{24N}{\omega^2} \int_{U_-}^0 \exp[\phi_N(U)] dU \times \int_{-\infty}^0 \exp[-\phi_N(\xi)] d\xi. \quad (\text{S.4})$$

Now the integrals are separate, we can evaluate them individually. In order to do this we use the Taylor expansions of  $\phi(U)$  around zero and  $U_-$ ;

$$\phi_N(U) \approx \phi_N(0) + U\phi'_N(0), \quad \phi_N(U) \approx \phi_N(U_-) + \frac{(U - U_-)^2}{2} \phi''_N(U_-).$$

Substituting  $U_- = -1$  and using the formula (S.3) we obtain, respectively:

$$\phi_N(U) \approx \frac{24N\beta}{\omega^2(1+\beta)} U, \quad \phi_N(U) \approx -\frac{12N\beta}{\omega^2(1+\beta)} + \frac{12N\beta}{\omega^2(1+\beta)} (U + 1)^2.$$

Substituting the first of these approximations in the first integral and the second approximation in the second integral in formula (S.4) we can extend the lower limit of the first integral to  $-\infty$

without considerably altering the integral. In a similar manner we can extend the upper limit of the second integral to  $\infty$ , to give an approximation to the switching time

$$T_1 \approx \frac{24N}{\omega^2} \int_{-\infty}^0 \exp\left[\frac{24N\beta}{\omega^2(1+\beta)}U\right] dU \times \int_{-\infty}^{\infty} \exp\left[\frac{12N\beta}{\omega^2(1+\beta)} - \frac{12N\beta}{\omega^2(1+\beta)}(U+1)^2\right] dU, \quad (\text{S.5})$$

which simplifies to

$$T_1 \approx \sqrt{\frac{\pi\omega^2(1+\beta)^3}{12\beta^3N}} \exp\left[\frac{12N\beta}{\omega^2(1+\beta)}\right]. \quad (\text{S.6})$$

From this equation we see that the mean switching time does not increase purely exponentially with the number of locusts: the exponential growth is slightly corrected by the inverse of a square root, which makes the growth of  $T_1$  as a function of  $N$  a little slower than exponential.

## S.2 Further analysis of the toy model

The Fourier transform of the probability distribution can be found as an infinite power series expansion in terms of the moments. It can be shown (again for the specific FPE [7]), as in (1), that there exists a recurrence relationship between the moments;  $T_n = n!T_1^n$ . Hence this power series can be expressed in terms of the first moment only:

$$\hat{P}(k) = \sum_{n=0}^{\infty} \frac{(ik)^n}{n!} T_n = \sum_{n=0}^{\infty} (ikT_1)^n = \frac{1}{1-ikT_1}. \quad (\text{S.7})$$

We can thus inverse-Fourier transform to obtain the probability distribution function

$$P(t) = \frac{1}{2\pi} \int_{-\infty}^{\infty} \frac{\exp(-ikT_1)}{1-ikT_1} dk = \frac{1}{T_1} \exp(-t/T_1). \quad (\text{S.8})$$

This distribution determines the probability that a switching event occurs between the time intervals  $t$  and  $t+dt$ . It only depends on the parameter  $T_1$  (mean switching time), the first moment of the distribution.

Since it is possible, in the locust experiment, to control environmental fluctuation, we can calculate what happens in the toy model if we add a source of environmental fluctuations to each of the equations of motion of the individual locusts. Assuming that these fluctuations are given by a Gaussian white noise  $\xi(t)$  with zero mean and correlation

$$\langle \xi(t)\xi(t') \rangle = \kappa^2\delta(t-t'), \quad (\text{S.9})$$

where  $\delta(x)$  is the Dirac delta function centered at  $x$ , we can repeat the arguments above to find the new probability distribution,

$$P^*(t) = \frac{1}{T_1^*} \exp(-t/T_1^*), \quad (\text{S.10})$$

where  $T_1^*$ , the mean switching time for the altered toy model, is given by

$$T_1^* = \sqrt{\frac{\pi(\omega^2 + 12\kappa^2)(1+\beta)^3}{12\beta^3N}} \exp\left[\frac{12N\beta}{(\omega^2 + 12\kappa^2)(1+\beta)}\right]. \quad (\text{S.11})$$

If we interpret  $\kappa$  as the control parameter, we can modify the first moment of the distribution (decreasing it) in a very efficient way; we cannot, however control the shape of the distribution.

### S.3 Choosing $\delta t$

The choice of  $\delta t$  is important when it comes to the accuracy of finding the drift and diffusion coefficients,  $F(U)$  and  $D(U)$  respectively, for the assumed underlying Fokker-Planck equation [12]. It turns out that the smaller (nonzero)  $\delta t$  is, the better the approximation to  $D(U)$  whereas the approximation to  $F(U)$  could be made worse. Both formulae [13] and [14], for  $F(U)$  and  $D(U)$  respectively, are true in the limit as  $\delta t \rightarrow 0$  if they are considered as averages over infinitely many realisations. However, when numerically approximating this limit can not actually be taken. The best we can do is to take a large but finite number of realisations and small  $\delta t$ . When considering experimental data the number of realisations possible is determined by the length of the obtained time series which is itself restricted by experimental time constraints. The appropriate choice of  $\delta t$  in the experimental situation will therefore depend on the number of available realisations as illustrated below.

Equation [12] can equivalently be written as a stochastic differential equation (SDE):

$$dU(t) = F(U(t))dt + \sqrt{2D(U(t))}dW, \quad (\text{S.12})$$

where  $dW$  is the standard Wiener process. To compute trajectories according to this equation one can use the Euler-Maruyama method:

$$U(t + \delta t) - U(t) = F(U(t))\delta t + \sqrt{2D(U(t))}\sqrt{\delta t} \Theta, \quad (\text{S.13})$$

where  $\Theta$  is a random number drawn from a normal distribution with zero mean and unit variance and  $\delta t$  is the time step. Substituting (S.13) into the right hand side of formula [13] gives

$$\left\langle \frac{U(t + \delta t) - U(t)}{\delta t} \right\rangle = \left\langle F(U(t)) + \frac{\sqrt{2D(U(t))}}{\sqrt{\delta t}} \Theta \right\rangle = F(U) + \frac{\sqrt{2D(U(t))}}{\sqrt{\delta t}} \langle \Theta \rangle, \quad (\text{S.14})$$

where  $\langle \cdot \rangle$  denotes the average over a finite number of realisations. If it were possible to take infinitely many realisations then the second term on the right hand side of equation (S.14) would disappear as  $\Theta$  is a random number sampled from a distribution with zero mean. In this case (S.14) is equivalent to formula [13]. In the case of finitely many realisations  $\langle \Theta \rangle$  is finite and non-zero (with probability 1), which means that taking very small values of  $\delta t$  magnifies the size of the second term in (S.14) leading to inaccuracies in our approximation of the drift coefficient. Proceeding in a similar manner for the diffusion coefficient; substituting from equation (S.13) into the right hand side of formula [14] leads to

$$\left\langle \frac{[U(t + \delta t) - U(t)]^2}{\delta t} \right\rangle = F(U(t))^2\delta t + 2F(U(t))\sqrt{2D(U(t))}\delta t\langle \Theta \rangle + 2D(U(t))\langle \Theta^2 \rangle. \quad (\text{S.15})$$

In the theoretical limit  $\delta t \rightarrow 0$  the first two terms disappear and (S.15) yields

$$\left\langle \frac{[U(t + \delta t) - U(t)]^2}{\delta t} \right\rangle = 2D(U(t))\langle \Theta^2 \rangle, \quad (\text{S.16})$$

which is equivalent to formula [14] providing we take (infinitely) many realisations (since  $\langle \Theta^2 \rangle = 1$  as  $\Theta$  is drawn from a distribution with unit variance and zero mean). Thus we see that the choice of a smaller  $\delta t$  reduces the error of the estimation of the diffusion coefficient. Using this rationale when simulating we used two different values of  $\delta t$  in order to find the most accurate approximations of the drift and diffusion coefficients. When finding the drift coefficient,  $F(U)$ , we used  $\delta t = 20 dt = 4$  seconds and when finding the diffusion coefficient,  $D(U)$ , we used  $\delta t = dt = 0.2$  seconds, where  $dt$  is the time period between recorded images (see Fig. 3).

## S.4 The experimental arena

The arena was composed of a ring-shaped flat and homogeneous formica sheet limited by an outer circular wall of 80 cm diameter and 52.5 cm high, coated with Fluon GP. A plastic hemisphere, 35 cm diameter, was coated with Fluon GP and placed at the centre of the arena, thus preventing locusts from seeing the movement of the locusts on the opposite side of the arena. Four high-frequency ‘daylight’ fluorescent tubes were placed 92.5 cm above forming a square tangent to the arena, which provided a bright and uniform lighting.

## S.5 Choice of $\eta$ for the revised model

In the original model  $\eta$  was chosen to be the constant unity. The experimental data indicate that the diffusion coefficient of the Fokker-Planck equation ([7] in the main text) is not, in fact, constant but appears to take a more quadratic form. We revised our model so that the noise term of an individual locust depended quadratically on group alignment, with high noise at low absolute alignment values and low noise at high absolute alignment values;

$$\eta(\bar{u}_i^{loc}) = C \left\{ 1 - \left( \frac{\bar{u}_i^{loc}}{|\bar{u}_i^{loc}|_{max}} \right)^2 \right\}, \quad (\text{S.17})$$

where  $C$  is a constant to be defined. We define the ‘total individual noise magnitude’ of the noise function  $\eta$  to be the integral from the minimum value of the local observable,  $\bar{u}_i^{loc}$ , to its maximum value. In order to give a fair comparison of the two models it was necessary to equate the total individual noise magnitudes of the two models:

$$\int_{-|\bar{u}_i^{loc}|_{max}}^{|\bar{u}_i^{loc}|_{max}} 1 \, d\bar{u}_i^{loc} = \int_{-|\bar{u}_i^{loc}|_{max}}^{|\bar{u}_i^{loc}|_{max}} C \left\{ 1 - \left( \frac{\bar{u}_i^{loc}}{|\bar{u}_i^{loc}|_{max}} \right)^2 \right\} d\bar{u}_i^{loc}. \quad (\text{S.18})$$

This leads to choosing  $C = 3/2$ .

## S.6 Additional figures

### S.6.1 Analysis of the toy model

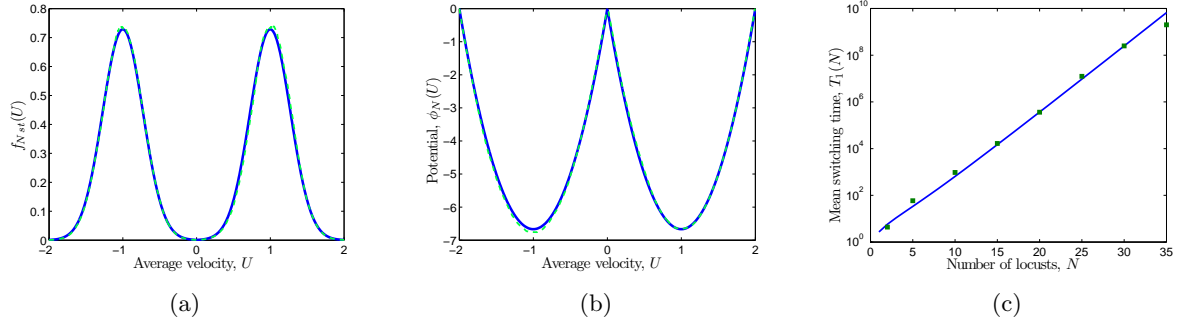


Figure S.1: Analysis of the global interaction model [5]. For  $\beta = 1$ ,  $\omega = 3$  and  $N = 10$  ((a) and (b) only). (a) The analytically derived SPD (solid line) of the approximate FPE for the average velocity, (see Eq. [6]) and the equation-free derived approximation to the SPD (dashed line). (b) The analytically derived potential (solid line) and the equation-free derived approximation to the potential (dashed line). (c) Mean switching time vs  $N$ : Analytically derived solution (solid line) and values simulated using the model [5] (squares). Note that there is a log-scale on the  $T_1$ -axis. In this global interaction case it is clear that the mean switching time increases exponentially with the number of locusts.

### S.6.2 Drift and potential for the local model

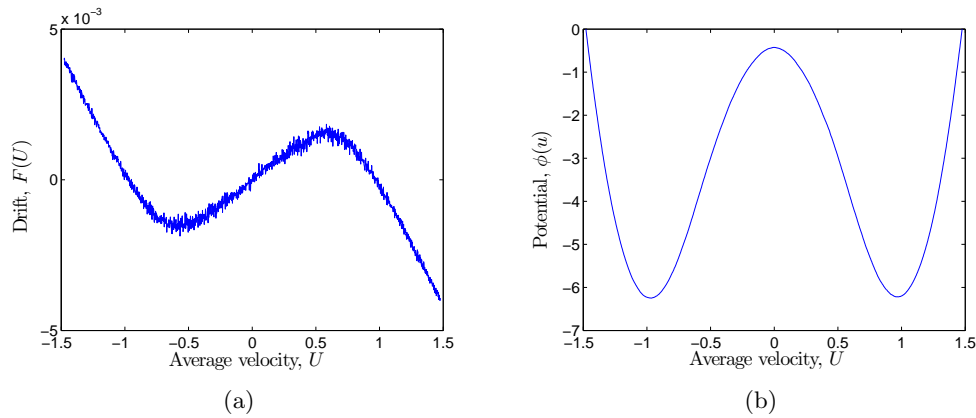


Figure S.2: Equation-free analysis of the local interaction model.  $L = 90$ ,  $R = 5$ ,  $\beta = 1$ ,  $\omega = 2.6$  and  $N = 30$ . Estimation of (a) the drift coefficient and (b) the potential of the unavailable FPE for the coarse variable,  $U$ .

### S.6.3 Potential for the experimental data

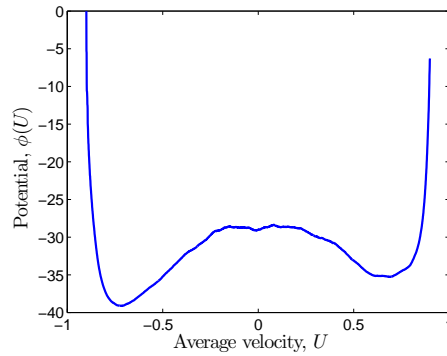


Figure S.3: Analysis of the experimental data. Potential of the unavailable FPE for the coarse variable,  $U$ , estimated using the systematic FPE coefficient estimation approach.

### S.6.4 Potential for the revised model

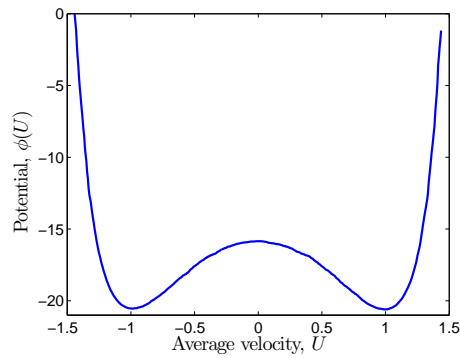


Figure S.4: Equation-free analysis of the revised local interaction model.  $L = 90$ ,  $R = 5$ ,  $\beta = 1$ ,  $\omega = 2.6$  and  $N = 30$ . Estimation of the potential of the unavailable FPE for the coarse variable,  $U$ .

## References

- [1] Fox R (1986) Functional-calculus approach to stochastic differential equations. *Phys Rev A* **33**(1) 467-476